Fig.1

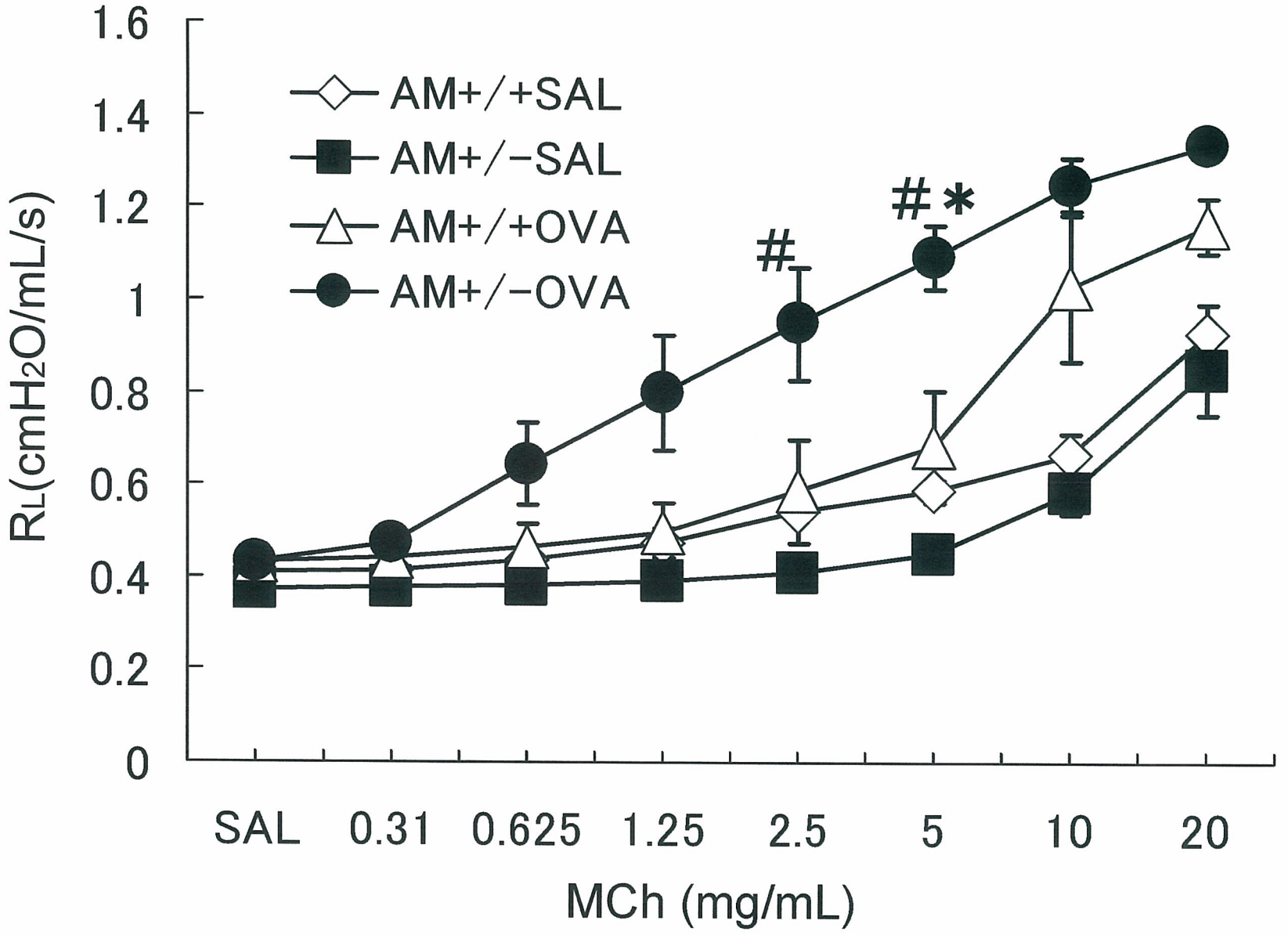
1.6
1.4
1.2
1
0.8
0.6
0.4
0.2
0
RL(cmH2O/mL/s)
AM+/+SAL
AM+/−SAL
AM+/+OVA
AM+/−OVA
#
#*
SAL
0.31
0.625
1.25
2.5
5
10
20
MCh (mg/mL)

Fig.2

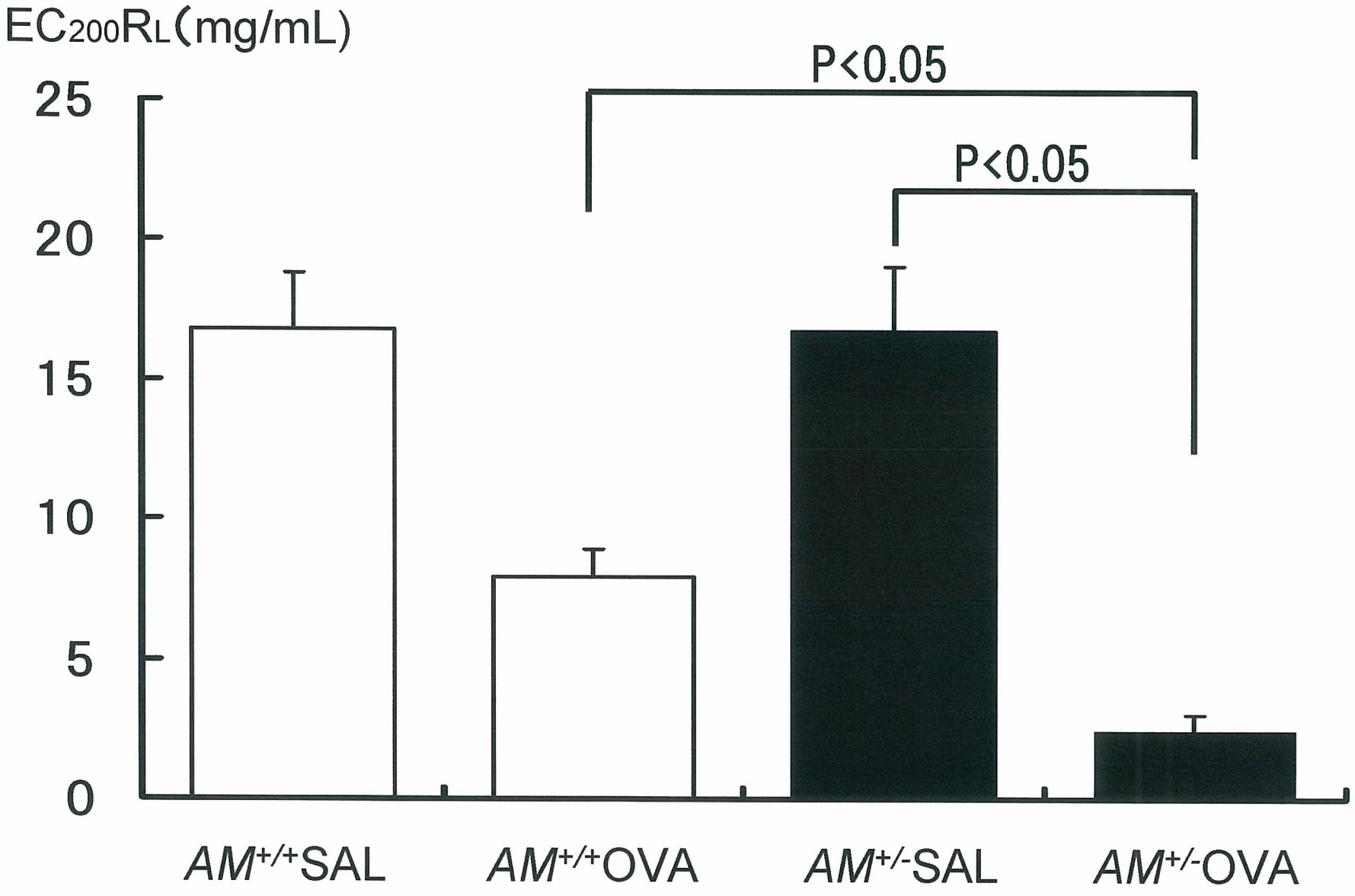

Fig.3

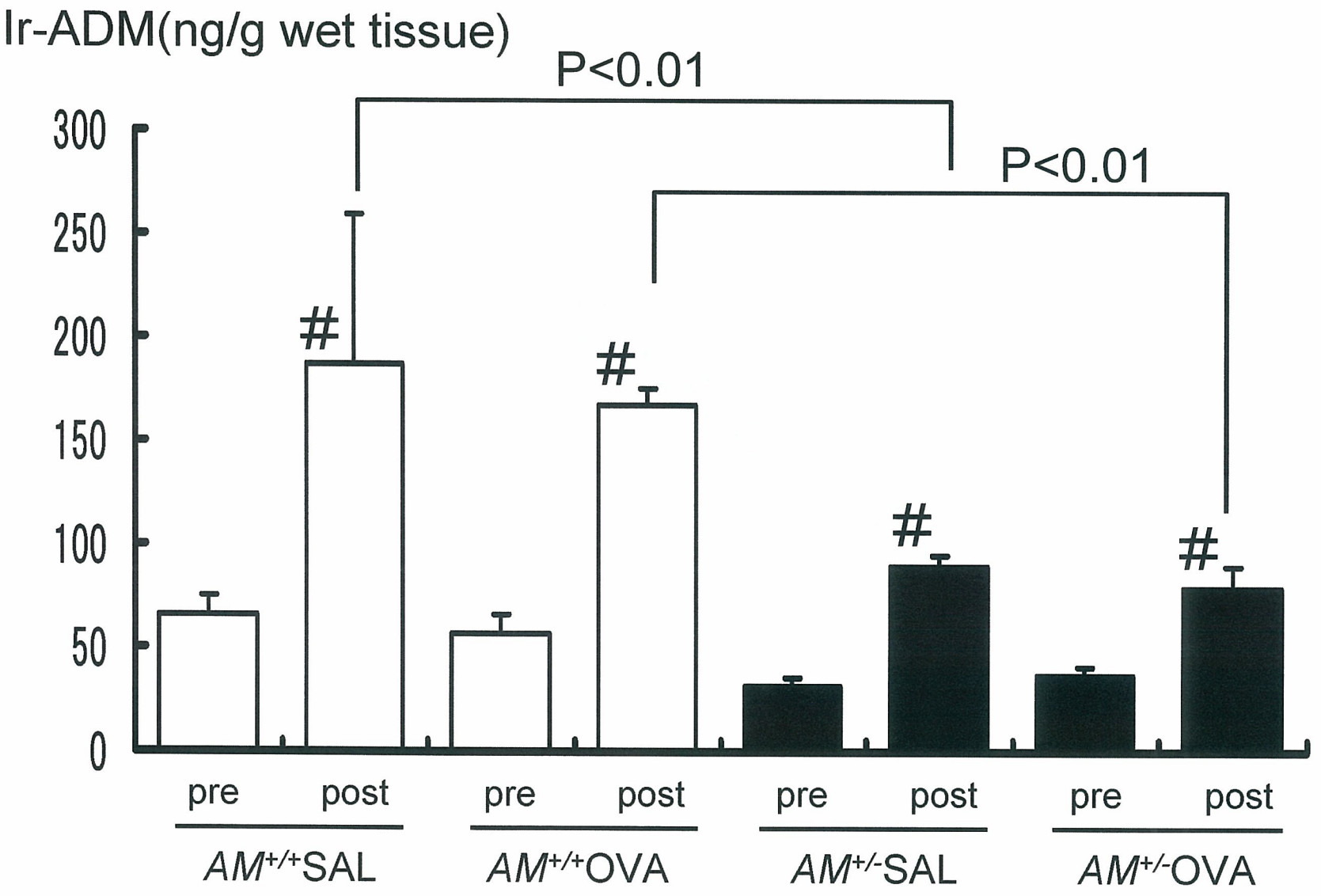
Ir-ADM(ng/g wet tissue)
P<0.01
P<0.01
300
250
200
150
100
50
0
#
#
#
#
pre
post
pre
post
pre
post
pre
post
AM+/+SAL
AM+/+OVA
AM+/-SAL
AM+/-OVA

Fig.4

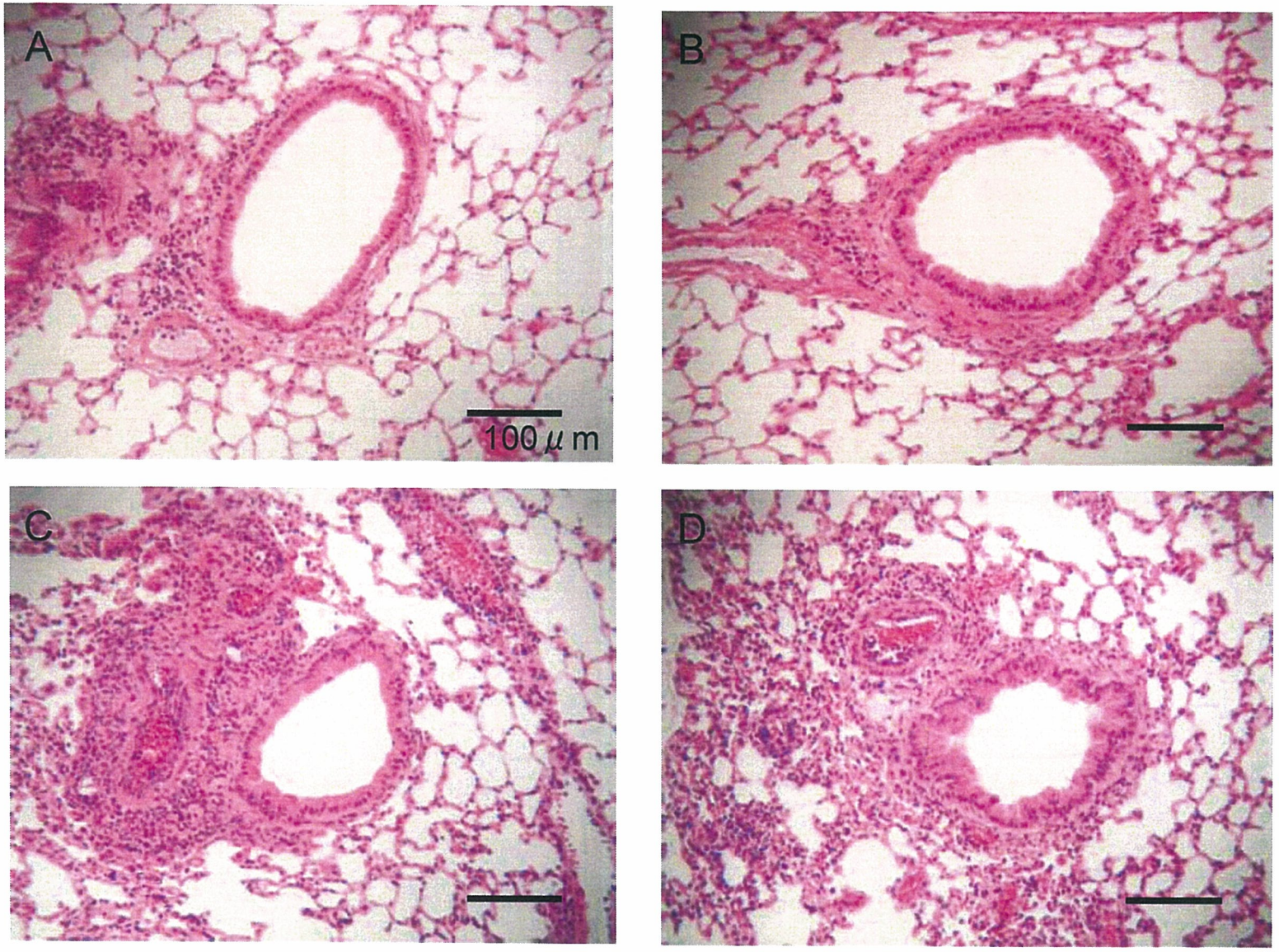

Fig.5

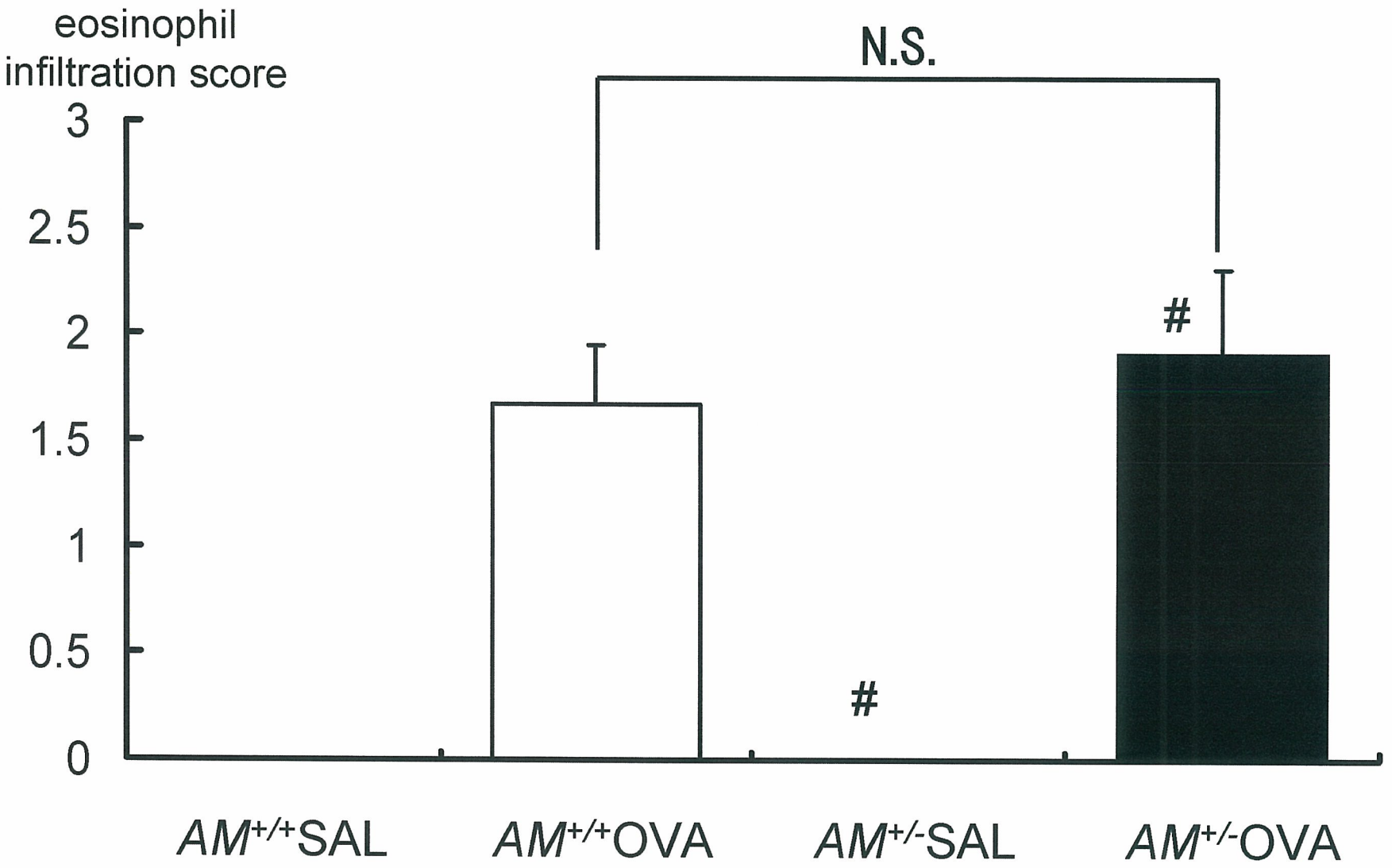
eosinophil
infiltration score
3
2.5
2
1.5
1
0.5
0
N.S.
#
#
AM+/+SAL
AM+/+OVA
AM+/-SAL
AM+/-OVA

Fig.6

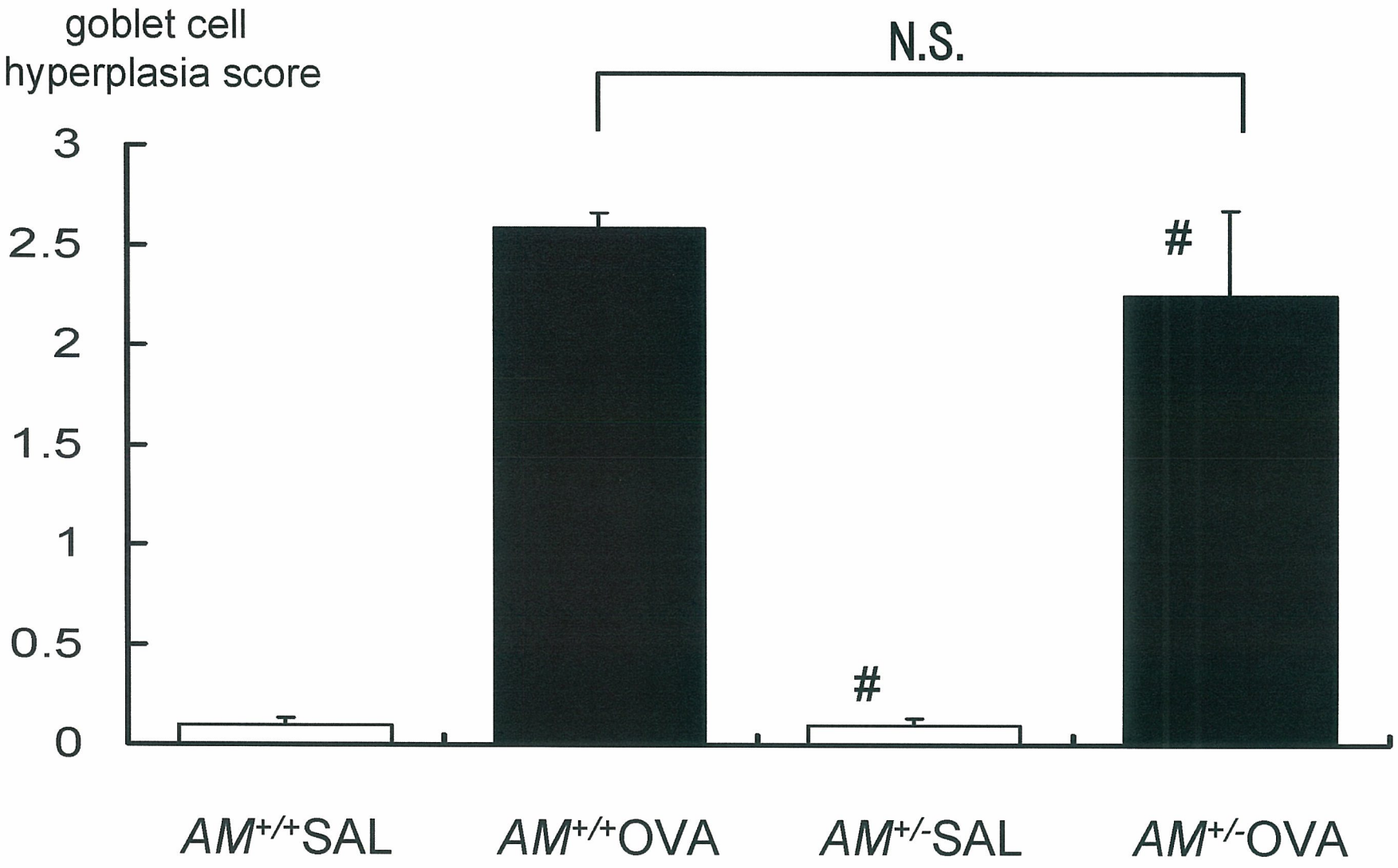
goblet cell
hyperplasia score
N.S.
3
2.5
2
1.5
1
0.5
0
#
#
AM+/+SAL
AM+/+OVA
AM+/-SAL
AM+/-OVA

Fig.7

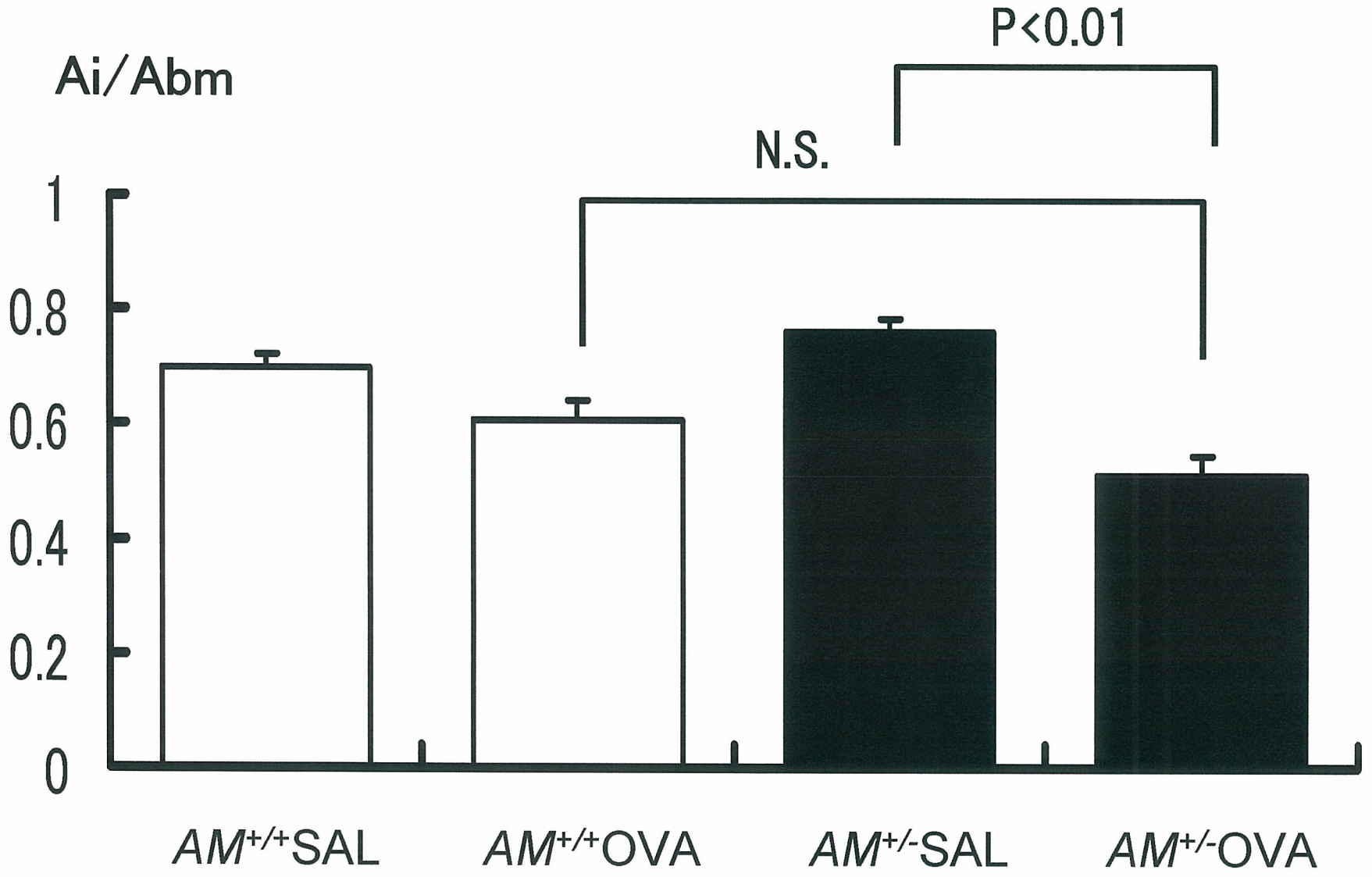

Fig.8

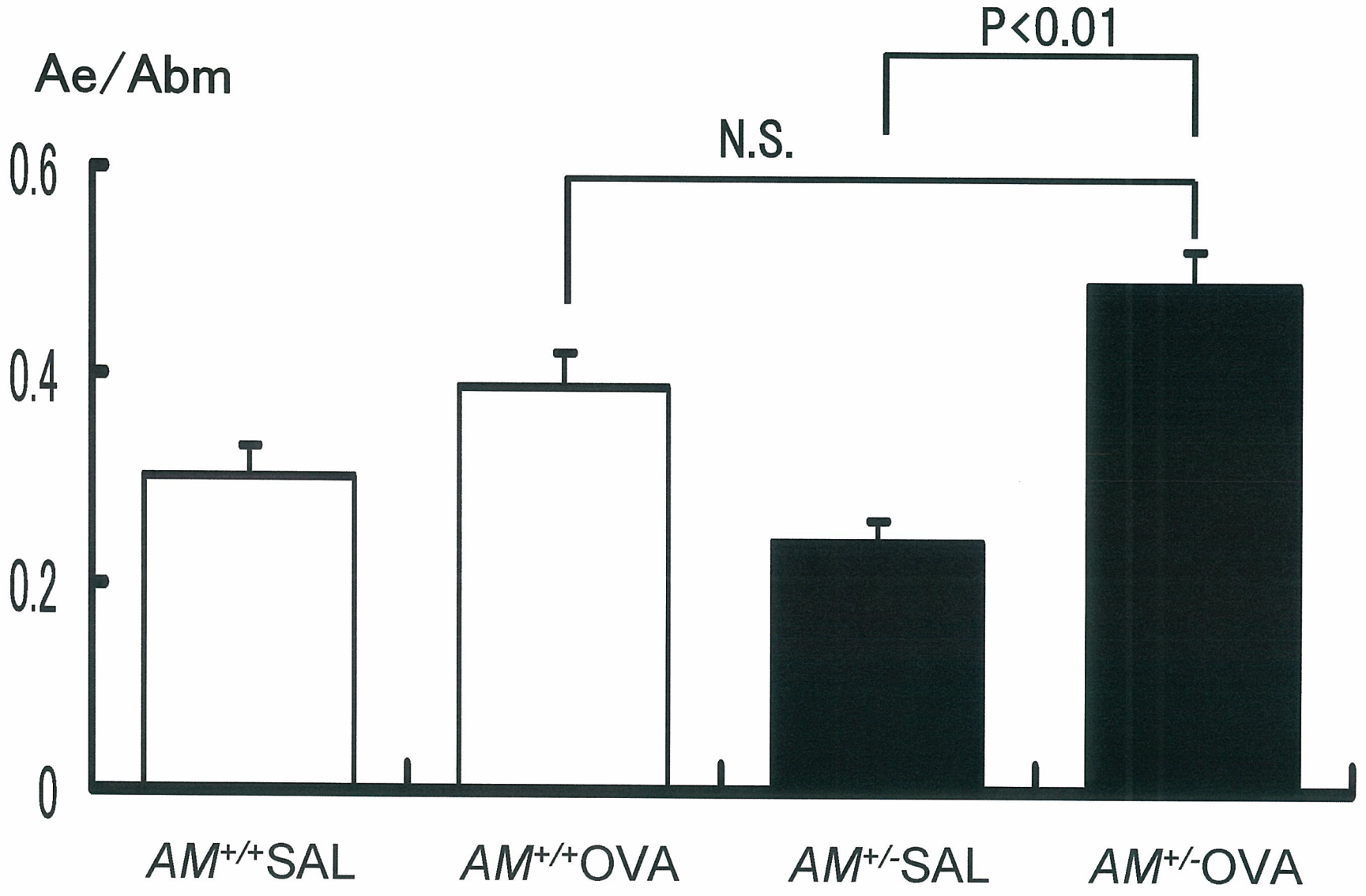

Fig.9

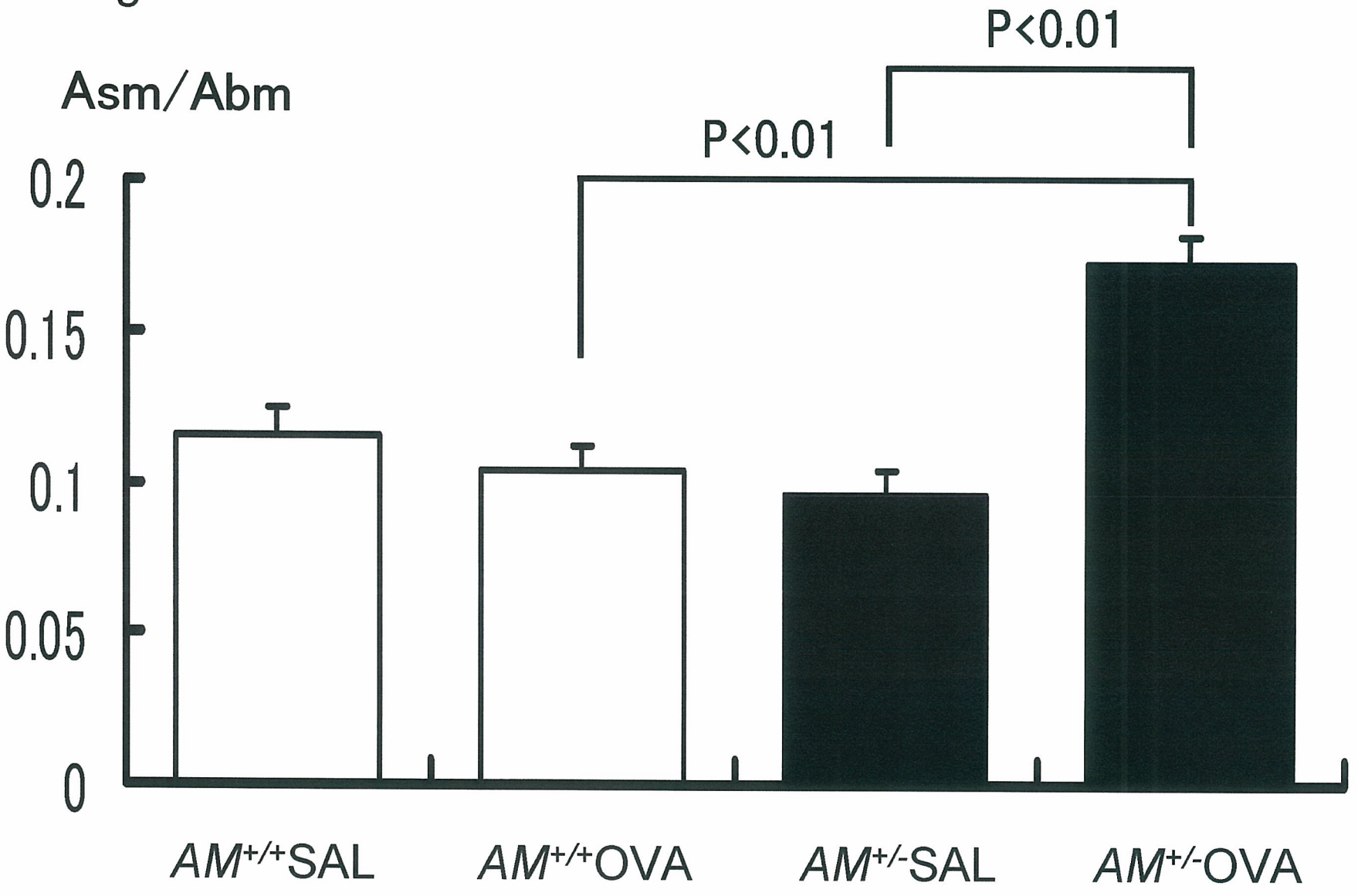

Fig.10

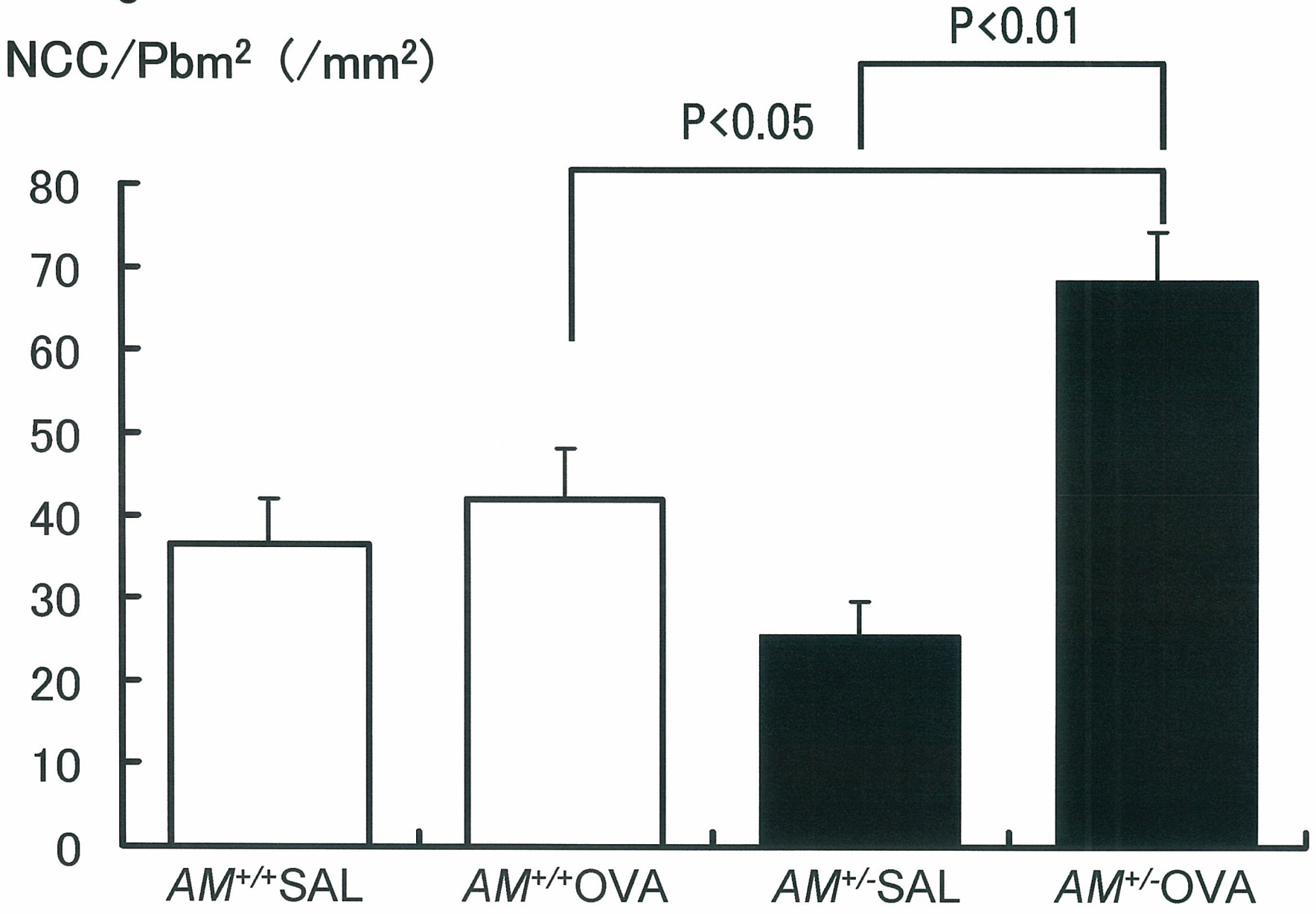
NCC/Pbm² (/mm²)
P<0.01
P<0.05
80
70
60
50
40
30
20
10
0
AM+/+SAL
AM+/+OVA
AM+/-SAL
AM+/-OVA

Fig.11

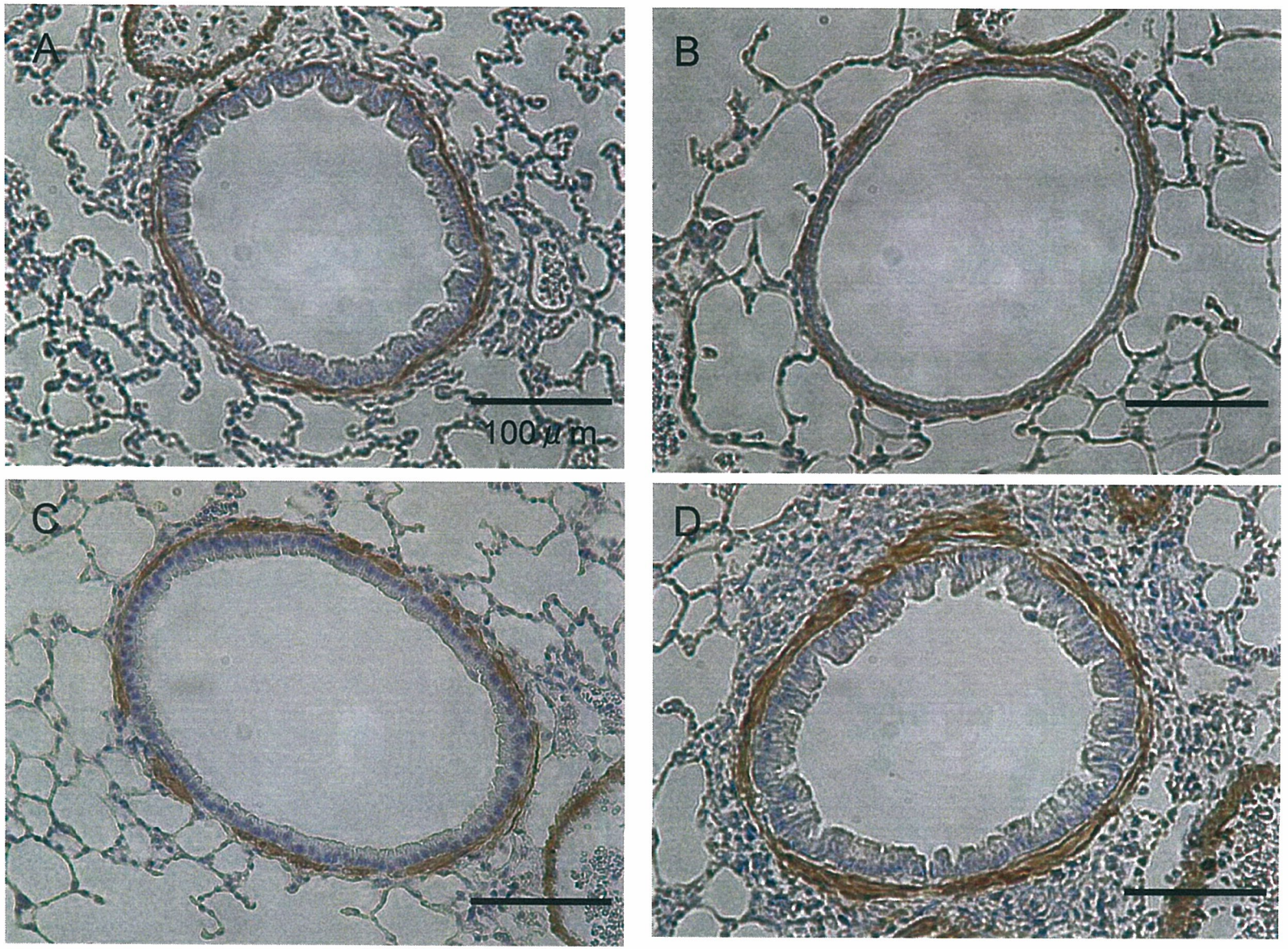

Fig.12

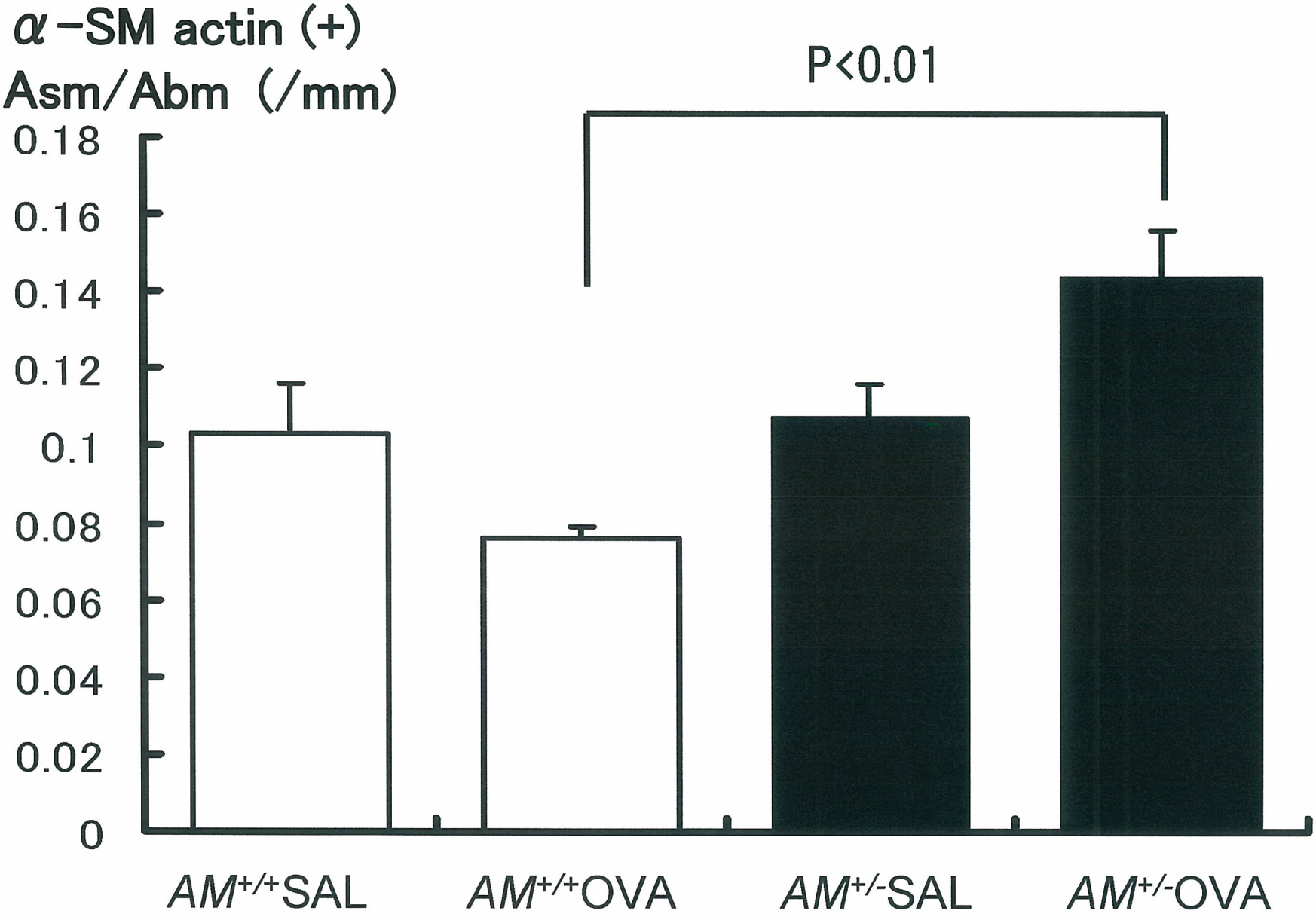
α-SM actin (+)
Asm/Abm (/mm)
P<0.01
0.18
0.16
0.14
0.12
0.1
0.08
0.06
0.04
0.02
0
AM+/+SAL
AM+/+OVA
AM+/-SAL
AM+/-OVA

Table 1. Total cell counts and cell fractions in BALF in each experimental group

	TCC ($x10^4$)	Mφ (%)	Lym (%)	Eos (%)	PMN (%)
***AM*$^{+/+}$Saline (n=5)**	4.94±1.91	96.02±2.82	4.32±2.67	0.02±0.00	0.26±0.21
***AM*$^{+/-}$Saline (n=5)**	4.82±0.54	91.96±2.51	7.24±2.25	0.10±0.00	0.82±0.48
***AM*$^{+/+}$OVA (n=5)**	40.20±18.22$^{\#}$	70.58±15.00	2.84±1.87	25.88±14.88*	0.72±0.45
***AM*$^{+/-}$OVA (n=6)**	21.13±8.75	60.02±12.41$^{\#}$	4.00±1.60	35.30±12.84$^{\#}$	0.70±0.28

Values are means ± SE, TCC: Total Cell Count, Mφ: Macrophages, Lym: Lymphocytes, Eos: Eosinophils, PMN: Polymorphonuclear cells

$^{\#}$P<0.05 compared with the saline group in the same strain of animals.

***P<0.01 compared with the saline group in the same strain of animals.**

Table 2. Biochemical analysis of BALF

	TP (μg/ml)	IgE (ng/ml)	IL-4 (pg/ml)	IL-5 (pg/ml)	IFN- γ (pg/ml)	LT C4/D4/E4 (pg/ml)
$AM^{+/+}$Saline (n=5)	4.94±1.91	5.30 ± 0.85	1092.3±17.1	17.0±3.8	1492.4±129.0	25.3±1.3
$AM^{+/-}$Saline (n=5)	4.82±0.54	4.44 ± 0.92	834.1±28.2	10.2±1.2	1548.4±119.2	4.3±0.5
$AM^{+/+}$OVA (n=9)	40.20±18.22	70.58±15.00	938.9±28.7	41.8±14.6	1353.0±66.6	41.4±26.4
$AM^{+/-}$OVA (n=7)	21.13±8.75	60.02±12.41	759.3±23.0	23.9±7.1	1624.3±119.2	15.6±4.8

Values are means ± SE, TP: Total Protein, IgE: Immunoglobulin E, IL-4: Interleukin-4, IL-5: Interleukin-5, IFN- γ: Interferon- γ, LT C4/D4/E4: Leukotriene C4/D4/E4

$^{\#}P<0.05$ compared with the saline group in the same strain of animals.

***P<0.01 compared with the saline group in the same strain of animals.**

Table 3. Immunoreactivity analysis of serum

	OVA-specific IgG1 (U/ml)	OVA-specific IgE (U/ml)
$AM^{+/+}$Saline	N.D.	N.D.
$AM^{+/-}$Saline	N.D.	N.D.
$AM^{+/+}$OVA	5578.4±4513.1 (n=6)	N.D.
$AM^{+/-}$OVA	1879.6±1389.3 (n=7)	N.D.

Values are means ± SE, N.D.: not detected

Am J Physiol Lung Cell Mol Physiol 290: L194–L199, 2006.
First published August 12, 2005; doi:10.1152/ajplung.00050.2005.

Involvement of the platelet-activating factor receptor in host defense against *Streptococcus pneumoniae* during postinfluenza pneumonia

Koenraad F. van der Sluijs,[1,2,3] Leontine J. R. van Elden,[4] Monique Nijhuis,[4] Rob Schuurman,[4] Sandrine Florquin,[5] Takao Shimizu,[6] Satoshi Ishii,[7] Henk M. Jansen,[2] René Lutter,[2,3] and Tom van der Poll[1]

[1]*Laboratory of Experimental Internal Medicine,* [2]*Department of Pulmonology,* [3]*Laboratory of Experimental Immunology,* [5]*Department of Pathology, Academic Medical Center, University of Amsterdam, Amsterdam;* [4]*Eijkman-Winkler Institute, Department of Virology, University Medical Center, Utrecht, The Netherlands;* [6]*Department of Biochemistry and Molecular Biology, Faculty of Medicine, The University of Tokyo; and* [7]*CREST of Japan Science and Technology Corporation, Tokyo, Japan*

Submitted 26 January 2005; accepted in final form 11 August 2005

van der Sluijs, Koenraad F., Leontine J. R. van Elden, Monique Nijhuis, Rob Schuurman, Sandrine Florquin, Takao Shimizu, Satoshi Ishii, Henk M. Jansen, René Lutter, and Tom van der Poll. Involvement of the platelet-activating factor receptor in host defense against *Streptococcus pneumoniae* during postinfluenza pneumonia. *Am J Physiol Lung Cell Mol Physiol* 290: L194–L199, 2006. First published August 12, 2005; doi:10.1152/ajplung.00050.2005.— Although influenza infection alone may lead to pneumonia, secondary bacterial infections are a much more common cause of pneumonia. *Streptococcus pneumoniae* is the most frequently isolated causative pathogen during postinfluenza pneumonia. Considering that *S. pneumoniae* utilizes the platelet-activating factor receptor (PAFR) to invade the respiratory epithelium and that the PAFR is upregulated during viral infection, we here used PAFR gene-deficient ($PAFR^{-/-}$) mice to determine the role of this receptor during postinfluenza pneumococcal pneumonia. Viral clearance was similar in wild-type and $PAFR^{-/-}$ mice, and influenza virus was completely removed from the lungs at the time mice were inoculated with *S. pneumoniae* (*day 14* after influenza infection). $PAFR^{-/-}$ mice displayed a significantly reduced bacterial outgrowth in their lungs, a diminished dissemination of the infection, and a prolonged survival. Pulmonary levels of IL-10 and KC were significantly lower in $PAFR^{-/-}$ mice, whereas IL-6 and TNF-α were only trendwise lower. These data indicate that the pneumococcus uses the PAFR leading to severe pneumonia in a host previously exposed to influenza A.

virus; bacteria; pneumonia; inflammation

ALTHOUGH INFLUENZA A INFECTION alone may lead to pneumonia, secondary bacterial infections during and shortly after recovery from influenza are much more common causes of pneumonia (12, 28). Bacteria such as *Staphylococcus aureus* and *Haemophilus influenzae* are known to cause postinfluenza pneumonia, but *Streptococcus pneumoniae* is the most prominent pathogen causing secondary bacterial pneumonia in recent decades (28). Primary infection with this pathogen is usually less severe than secondary infection (16). Influenza is known to increase adherence of and subsequent colonization with bacterial respiratory pathogens. Bacteria may adhere to the basal membrane after disruption of the airway epithelial layer by the cytopathic effect of the virus (17) but may also bind to specific receptors in the airway epithelium induced by influenza virus (6, 11). Because the platelet-activating factor receptor (PAFR) has been described to be upregulated during viral infections (10) and since the PAFR is able to bind phosphorylcholine, a cell wall component of *S. pneumoniae* (3, 5, 12), it has been suggested that the PAFR may play a critical role during secondary bacterial pneumonia (11).

The PAFR, a G protein-coupled receptor, is mainly expressed on macrophages, monocytes, neutrophils, and epithelial cells (8, 9, 22, 24). Activation of epithelial cells leads to upregulation of the PAFR at the cell surface, which facilitates colonization and invasion of *S. pneumoniae* (3, 9). A recent study by McCullers and Rehg (11) investigated the potential role of the PAFR in pneumococcal pneumonia following influenza A infection. These authors showed that PAFR blockade during secondary pneumococcal pneumonia does not prevent lethal synergism between influenza virus and *S. pneumoniae* (11). Moreover, administration of the PAFR antagonist CV-6209 resulted in enhanced bacterial outgrowth, even in mice with primary pneumococcal pneumonia (11). These findings contrast with earlier studies reporting that administration of PAFR antagonists reduced pneumococcal outgrowth in rabbits (2, 3). In line, our laboratory recently demonstrated that PAFR gene deficient ($PAFR^{-/-}$) mice display a diminished bacterial outgrowth and a reduced lethality after intranasal infection with *S. pneumoniae* (20). To obtain further insight in the role of the PAFR during secondary bacterial pneumonia, we inoculated $PAFR^{-/-}$ mice and wild-type mice with *S. pneumoniae* on *day 14* after influenza virus infection and studied host defense against primary influenza virus infection and secondary *S. pneumoniae* infection.

MATERIALS AND METHODS

Mice. $PAFR^{-/-}$ mice were generated as described (7) and backcrossed seven times to a C57BL/6 background. Wild-type C57BL/6 mice were obtained from Harlan Sprague-Dawley. Pathogen-free 8-wk-old female C57BL/6 mice and $PAFR^{-/-}$ mice were maintained at biosafety *level 2* during the experiments. All experiments were approved by the Institutional Animal Care and Use Committee of the Academic Medical Center.

Experimental infection protocol. Influenza A/PR/8/34 (VR-95; ATCC, Rockville, MD) was grown on LLC-MK2 cells (RIVM,

Address for reprint requests and other correspondence: K. van der Sluijs, Laboratory of Experimental Immunology, Rm. G1-140, Academic Medical Center, Meibergdreef 9, 1105 AZ, Amsterdam, The Netherlands (e-mail: kvandersluijs@amc.uva.nl).

The costs of publication of this article were defrayed in part by the payment of page charges. The article must therefore be hereby marked "*advertisement*" in accordance with 18 U.S.C. Section 1734 solely to indicate this fact.

Bilthoven, Netherlands). Virus was harvested by a freeze-thaw cycle, followed by centrifugation at 680 *g* for 10 min. Supernatants were stored in aliquots at −80°C. Titration was performed in LLC-MK2 cells to calculate the median tissue culture infective dose ($TCID_{50}$) of the viral stock (18). A noninfected cell culture was used for preparation of the control inoculum. None of the stocks were contaminated by other respiratory viruses, i.e., influenza B; human parainfluenza type 1, 2, 3, 4A, and 4B; Sendai virus; respiratory syncytial virus A and B; rhinovirus; enterovirus; corona virus; and adenovirus; as determined by PCR or cell culture. Viral stock and control stock were diluted just before use in phosphate-buffered saline (PBS, pH 7.4). Primary influenza infection and secondary pneumococcal pneumonia were induced according to previously described methods (30, 31). In brief, mice were anesthetized by inhalation of isoflurane (Abbott Laboratories, Kent, UK) and intranasally inoculated with 10 $TCID_{50}$ influenza (1,400 viral copies) or control inoculum in a final volume of 50 μl of PBS. Pneumococcal pneumonia was induced 14 days after inoculation with influenza or control suspension. *S. pneumoniae serotype 3* (ATCC 6303) was cultured for 16 h at 37°C in 5% CO_2 in Todd Hewitt broth. This suspension was diluted 100 times in fresh medium and grown for 5 h to midlogarithmic phase. Bacteria were harvested by centrifugation at 2,750 *g* for 10 min at 4°C and washed twice with ice-cold saline. After the second wash, bacteria were resuspended in saline and diluted to a concentration of 2×10^5 colony forming units (CFU) per ml, which was verified by plating out 10-fold dilutions onto blood-agar plates. Mice were anesthetized by inhalation with isoflurane and were inoculated with 50 μl of the bacterial suspension (10^4 CFU *S. pneumoniae*).

Determination of PAFR expression in the lungs. The expression of the PAFR in the lungs was determined on *day 8* and *day 14* after influenza virus infection. Mice (eight per time point) were anesthetized with 0.3 ml FFM (0.079 mg/ml fentanyl citrate, 2.5 mg/ml fluanisone, and 1.25 mg/ml midazolam in H_2O; of this mixture 7.0 ml/kg intraperitoneally) and killed by bleeding out the vena cava inferior. Lungs were harvested and homogenized at 4°C in four volumes of sterile saline with a tissue homogenizer (Biospec Products, Bartlesville, OK). Hundred microliters of lung homogenates were treated with 1 ml of TRIzol reagent to extract RNA. RNA was resuspended in 10 μl of diethyl pyrocarbonate-treated water. cDNA synthesis was performed using 1 μl of the RNA suspension and a random hexamer cDNA synthesis kit (Applera, Foster City, CA). Two microliters out of 20 μl of cDNA suspension were used for amplification in real-time quantitative PCR reaction (Lightcycler Sequence Detector System; Roche, Mannheim, Germany). A standard curve was made using 10-fold dilutions of cDNA obtained from influenza virus-infected lung material. PAFR mRNA expression levels were normalized for the amount of TATA-box binding protein (TBP) mRNA present in each sample (1). The following primers were used: 5′-CTGGACCCTAGCAGAGTTGG-3′ (forward) and 5′-GCTACTGCGCATGCTGTAAA-3′ (reverse) for PAFR, 5′-CAGGAGCCAAGAGTGAAGAAC-3′ (forward) and 5′-GGAAATAATTCTGGCTCATAGCTACT-3′ (reverse) for TBP.

Determination of viral load in the lungs. Viral load was determined on *days 8* and *14* after viral infection and 48 h after pneumococcal infection (i.e., 16 days after viral infection) using real-time quantitative PCR as described (30, 31, 32). Five microliters out of 25 μl of cDNA suspension were used for amplification in a quantitative real-time PCR reaction (ABI PRISM 7700 Sequence Detector System). The viral load present in each sample was calculated with a standard curve of particle-counted influenza virus (virus particles were counted by electron microscopy), included in every assay. The following primers were used: 5′-GGACTGCAGCTGAGACGCT-3′ (forward); 5′-CATCCTGTTGTATATGAGGCCCAT-3′ (reverse) and 5′-CTCAGTTATTCTGCTGGTGCACTTGCC-3′ (5′-FAM-labeled probe).

Determination of bacterial outgrowth. Serial 10-fold dilutions of the lung homogenates in sterile saline and 10-μl volumes were plated out onto blood-agar plates. Plates were incubated at 37°C at 5% CO_2, and CFUs were counted after 16 h.

Histopathological analysis. Lungs for histological examination were harvested 48 h after pneumococcal infection, fixed in 10% formalin, and embedded in paraffin. Sections (4 μm) were stained with hematoxylin and eosin (H/E) and analyzed by a pathologist who was blinded for the groups.

Bronchoalveolar lavage. The trachea was exposed through a midline incision and cannulated with a sterile 22-gauge Abbocath-T catheter (Abbott, Sligo, Ireland). Bronchoalveolar lavage (BAL) was performed by instillation of two 0.5-ml aliquots of sterile saline into the right lung. The retrieved BAL fluid (BALF, ~0.8 ml) was spun at 260 *g* for 10 min at 4°C, and the pellet was resuspended in 0.5 ml of sterile PBS. Total cell numbers were counted using a Z2 Coulter Particle Count and Size Analyzer (Beckman-Coulter, Miami, FL). Differential cell counts were done on cytospin preparations stained with modified Giemsa stain (Diff-Quick, Baxter, UK).

Cytokine and chemokine measurements. Lung homogenates were lysed with an equal volume of lysis buffer [300 mM NaCl, 30 mM Tris, 2 mM $MgCl_2$, 2 mM $CaCl_2$, 1% (vol/vol) Triton X-100, 20 ng/ml pepstatin A, 20 ng/ml leupeptin, and 20 ng/ml aprotinin, pH 7.4] and incubated for 30 min on ice, followed by centrifugation at 680 *g* for 10 min. Supernatants were stored at −80°C until further use. Cytokines and chemokines in total lung lysates were measured by enzyme-linked immunosorbent assay according to the manufacturer's protocol. Reagents for interleukin (IL)-6, IL-10, cytokine-induced neutrophil chemoattractant (KC), and tumor necrosis factor (TNF)-α measurements were obtained from R&D systems (Abingdon, UK); interferon-γ reagents were obtained from Pharmingen (San Diego, CA).

Statistical analysis. All data are expressed as means ± SE, unless stated otherwise. Differences between groups were analyzed by Mann-Whitney *U*-test. Survival was analyzed with Kaplan-Meier using a log-rank test; $P < 0.05$ was considered to represent a statistically significant difference.

RESULTS

PAFR expression in the lungs after influenza virus infection in mice. PAFR expression in the lungs was determined by real-time PCR on *day 8* and *day 14* after influenza virus infection. A 10-fold increase in PAFR mRNA was observed on *day 8* after viral infection ($P = 0.0095$ vs. control mice, Fig. 1).

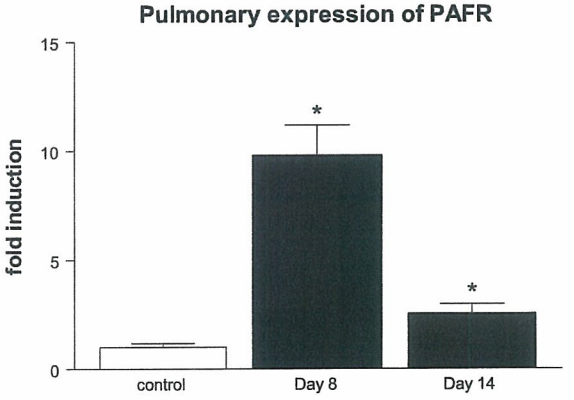

Fig. 1. Pulmonary expression of platelet-activating factor receptor (PAFR) after influenza virus infection. PAFR mRNA was measured by real-time quantitative PCR (8 mice per time point), except control group (4 mice). Expression levels were normalized for TATA-box binding protein mRNA expression levels. Data are expressed as fold induction over control (± SE). *$P < 0.05$ vs. control mice.

Although the expression of the PAFR declined thereafter, a 2.5-fold increase could still be observed on *day 14* after viral infection ($P = 0.0162$ vs. control mice). These data indicate that influenza virus induces the expression of PAFR in vivo.

Primary influenza virus infection. Viral load in the lungs was measured on *day 8* and *day 14* after infection to determine the role of the PAFR during primary influenza A infection. Viral load was similar in PAFR$^{-/-}$ and wild-type mice on *day 8* after infection (Fig. 2). On *day 14* after infection, both wild-type and PAFR$^{-/-}$ mice had cleared the virus completely. These data indicate that PAFR deficiency does not hamper the clearance of influenza A in vivo.

Prolonged survival during secondary pneumococcal infection in PAFR$^{-/-}$ mice. To investigate the role of the PAFR during secondary bacterial pneumonia we inoculated mice with *S. pneumoniae* on *day 14* after influenza infection. Lethality was monitored in PAFR$^{-/-}$ and wild-type mice (11 mice per group) during secondary pneumococcal pneumonia at least twice daily (Fig. 3). Influenza-recovered PAFR$^{-/-}$ mice displayed a prolonged survival after pneumococcal infection ($P = 0.014$ vs. wild-type mice).

Bacterial outgrowth. To obtain insight into the role of the PAFR in the outgrowth of pneumococci in lungs previously exposed to influenza A and in the dissemination of bacteria, lungs and blood were cultured 48 h after infection with *S. pneumoniae*. The number of *S. pneumoniae* CFU was threefold lower in PAFR$^{-/-}$ than in wild-type mice ($P = 0.05$, Fig. 4). Moreover, the PAFR played a role in the dissemination of *S. pneumoniae* into the circulation: only 57% of PAFR$^{-/-}$ mice had positive blood cultures vs. 100% of wild type, and the number of *S. pneumoniae* CFU in blood of PAFR$^{-/-}$ mice was lower than in wild-type mice ($P = 0.05$, Fig. 4).

Pulmonary cytokine and chemokine concentrations. Cytokines and chemokines play an important role in host defense against bacterial pneumonia (26). Therefore, to determine the effect of the PAFR on the induction of these mediators, the concentrations of TNF-α, IL-6, IL-10, and KC were measured in lung homogenates (Fig. 5). Lung levels of TNF-α, IL-6, and IL-10 were similar in wild-type mice and PAFR$^{-/-}$ mice on *day 14* after influenza infection (Fig. 5), whereas KC production was slightly reduced in PAFR$^{-/-}$ mice ($P = 0.0317$ vs. wild-type mice). *S. pneumoniae* infection on *day 14* after influenza resulted in enhanced production of TNF-α, IL-6, IL-10, and KC (Fig. 5). On *day 16*, i.e., 48 h after *S. pneumoniae* infection, IL-10 and KC levels were significantly lower in PAFR$^{-/-}$ mice than in wild-type mice ($P < 0.05$). Lung levels of TNF-α and IL-6 tended to be lower in PAFR$^{-/-}$ mice, but the difference with wild-type mice was not statistically significant ($P = 0.16$ and $P = 0.09$ respectively).

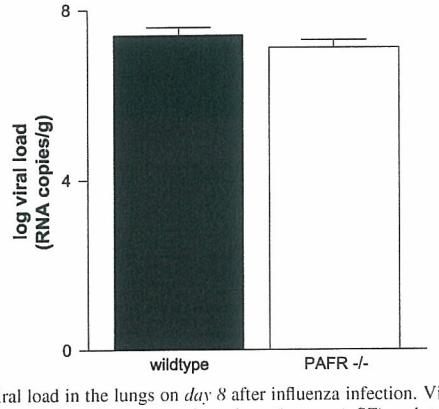

Fig. 2. Viral load in the lungs on *day 8* after influenza infection. Viral load is expressed as RNA copies per gram lung tissue (means ± SE) as determined by real-time PCR (5–8 mice per group). Both wild-type mice (filled bar) and PAFR$^{-/-}$ mice (open bar) had cleared the virus on *day 14* after infection (data not shown).

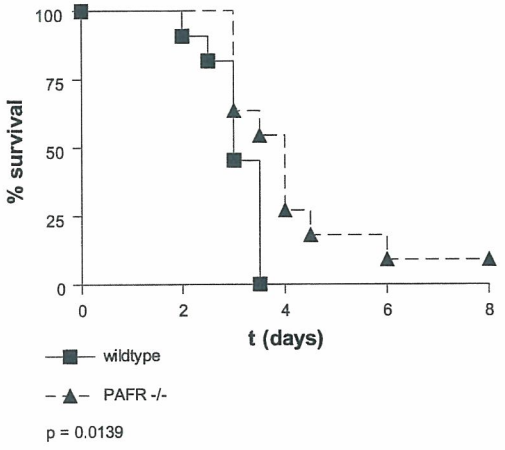

Fig. 3. Prolonged survival in PAFR$^{-/-}$ mice after secondary bacterial pneumonia. Survival after pneumococcal infection in influenza-recovered PAFR$^{-/-}$ mice (▲) vs. wild-type mice (■). All mice (11 mice per group) received 10^4 colony-forming units (CFU) of *Streptococcus pneumoniae* on *day 14* after viral infection and were monitored at least twice a day after pneumococcal infection.

Cell influx in BALF. Neutrophils play a pivotal role in host defense against bacterial pneumonia (26). Because inhibition of PAFR function has been shown to reduce leukocyte influx into the lungs in response to intrapulmonary delivery of killed pneumococci (16), we assessed the number of leukocytes recruited to the alveoli. Although total cell counts tended to be lower in BALF obtained from PAFR$^{-/-}$ mice than in BALF from wild-type mice, this difference was not statistically significant. The relative number of neutrophils was trendwise lower in PAFR$^{-/-}$ mice ($P = 0.09$ vs. wild-type mice, Table 1), whereas the relative number of macrophages was trendwise higher in PAFR$^{-/-}$ mice ($P = 0.09$ vs. wild-type mice, Table 1).

Histopathology. Forty-eight hours after pneumococcal infection, lungs were harvested to prepare H/E-stained lung slides for histopathological examination. Mice recovered from influenza infection with secondary pneumococcal pneumonia showed severe interstitial inflammation, bronchiolitis, endothelialitis, and pleuritis in the lungs. No significant differences were observed between wild-type mice and PAFR$^{-/-}$ mice (Fig. 6).

DISCUSSION

Secondary pneumococcal pneumonia is a serious complication of influenza A infection. The increased susceptibility to secondary bacterial infections during and shortly after influenza is, at least in part, due to enhanced colonization and interaction of the respiratory epithelium with *S. pneumoniae*

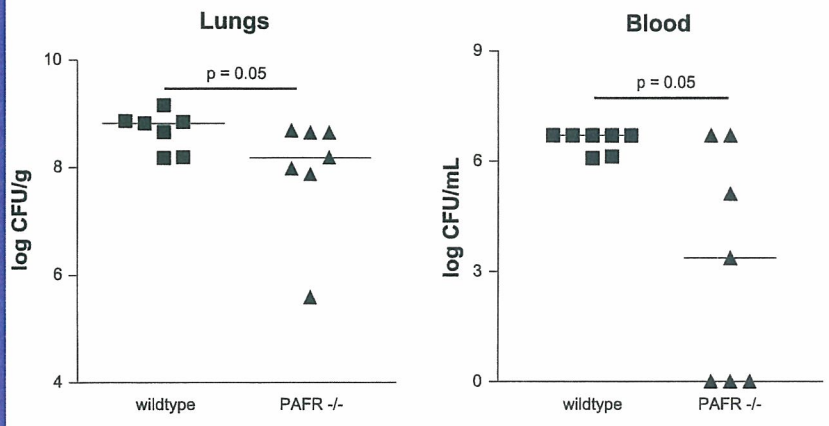

Fig. 4. Reduced bacterial outgrowth in the lungs and blood of PAFR$^{-/-}$ mice. Bacterial outgrowth in the lungs (*left*) and blood (*right*) after pneumococcal infection in wild-type mice (■) and PAFR$^{-/-}$ mice (▲). All mice (7 mice per group) received 10^4 CFU *S. pneumoniae* on *day 14* after viral infection and were killed 48 h later. Horizontal lines represent medians for each group. Note that 3 PAFR$^{-/-}$ mice had no bacteria in their blood 48 h after infection.

(14, 16, 28). Because the PAFR has been described to be upregulated during viral infections (10) and since the PAFR facilitates invasion of the pneumococcus through epithelial cells through binding of phosphorylcholine in the cell wall of *S. pneumoniae* (3), it has been suggested that the PAFR may play a critical role during postinfluenza pneumococcal pneumonia (11). In the present study we show that influenza virus infection in mice results in increased PAFR expression in the lungs on *day 8* and *day 14* after infection. In addition, targeted deletion of the PAFR improves host defense against *S. pneumoniae* in a mouse model for secondary bacterial pneumonia, as reflected by prolonged survival and reduced bacterial loads in the lungs and the circulation.

Our data are contradictory to a previous study by McCullers and Rehg (11), who showed that influenza-infected mice treated with CV-6209, a PAFR antagonist, displayed enhanced outgrowth of pneumococci (72 h after infection). Although several differences between our investigation and that of McCullers and Rehg (11) can be pointed out, including differences in the *S. pneumoniae* strains used (ATCC 6303, *serotype 3* vs. D39, *serotype 2*, respectively) and differences in the interval between influenza and secondary pneumococcal infection (14 vs. 7 days, respectively), the data reported by McCullers and Rehg are difficult to explain in the context of current knowledge on the role of the PAFR in pneumococcal infection. Indeed, these authors observed a reduced rather than an increased host defense after administration of a PAFR antagonist during primary pneumococcal pneumonia (10), which contrasts with three earlier investigations addressing this topic (2, 3, 20). Our own laboratory found that PAFR$^{-/-}$ mice display enhanced survival and reduced bacterial outgrowth after primary pneumococcal pneumonia (20). Similarly, intratracheal PAFR antagonist treatment during pneumococcal infection in rabbits resulted in reduced bacterial loads in the lung (3). Conceivably, the specific properties of the PAFR antagonist used by McCullers and Rehg (11) may have played a role. Hence, our current data seem to indicate that the pneumococcus uses the PAFR to invade the respiratory epithelium of the

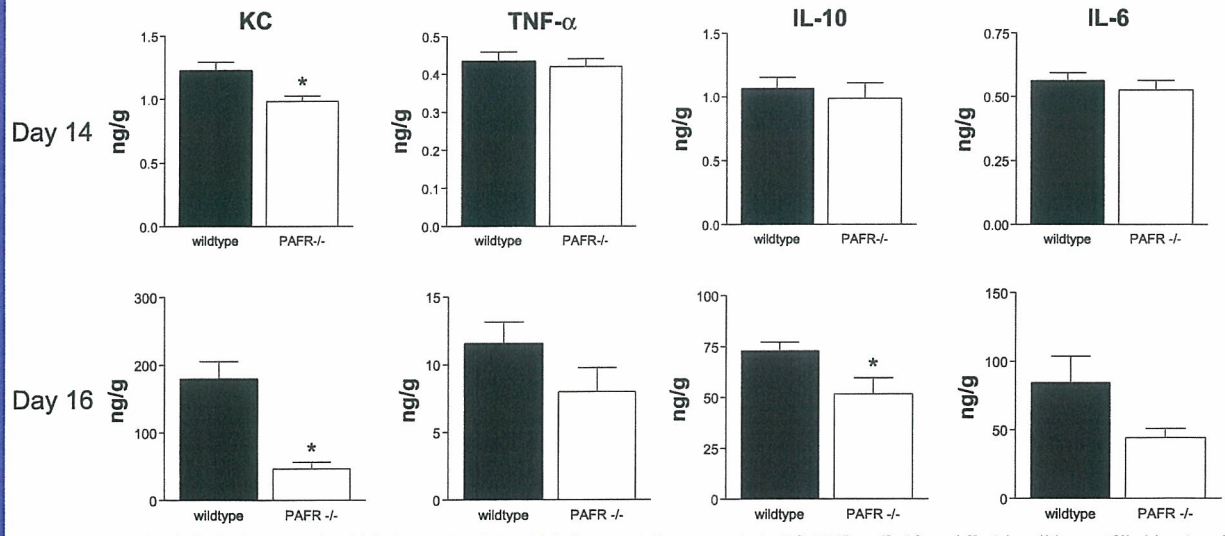

Fig. 5. Cytokine levels in the lungs on *day 14* (influenza) and *day 16* (influenza + *S. pneumoniae*): KC, TNF-α, IL-10, and IL-6 in wild-type (filled bars) and PAFR$^{-/-}$ mice (open bars) at 48 h after secondary bacterial pneumonia. Data are expressed in ng/g lung tissue (means ± SE, 5–7 mice per group). Please note that the *x*-axis scales differ between the *top* and *bottom* panels (mediator levels before bacterial pneumonia were much lower). *$P < 0.05$ vs. wild-type mice

Table 1. *Leukocytes in BALF 48 h after secondary bacterial pneumonia*

Cells, $\times 10^3$	Wild-type Mice	PAFR$^{-/-}$ Mice
Total cell count	1,398±411	782±335
Neutrophils (%)	1,046±325 (67.2%)	458±184 (52.5%)
Macrophages (%)	336±98 (31.5%)	321±164 (46.8%)
Lymphocytes (%)	16.2±9.8 (1.3%)	2.9±1.5 (0.7%)

Leukocyte counts (6 mice per group) are expressed as absolute numbers ($\times 10^3$) and percentages of total cell count. All data are means ± SE. No statistically significant differences were found between wild-type and PAFR$^{-/-}$ mice 48 h after secondary pneumococcal pneumonia. PAFR, platelet-activating factor receptor; BALF, bronchoalveolar lavage fluid.

host previously exposed to influenza A. As such, the involvement of the PAFR in the pathogenesis of primary and postinfluenza pneumococcal pneumonia seems quite similar (20).

Of note, in our study, an interval of 14 days between viral and bacterial infection was chosen to exclude a direct interaction between influenza virus and *S. pneumoniae*. Previous studies by our group have indicated that influenza virus is completely cleared from the lungs of wild-type mice on *day 14* after infection (32), which was confirmed here. The present study establishes that clearance of influenza A is not altered in PAFR$^{-/-}$ mice: viral loads were similar in PAFR$^{-/-}$ and wild-type mice 8 days after infection and both strains had cleared the virus completely on *day 14*, the day on which pneumococcal pneumonia was induced. These findings not only revealed that the PAFR does not contribute to host defense against influenza A to a significant extent but also allowed us to use PAFR$^{-/-}$ mice to study the role of the PAFR during postinfluenza pneumococcal pneumonia.

The improved outcome observed in PAFR$^{-/-}$ mice could also be explained by the release of protective mediators after pneumococcal infection. Pulmonary levels of KC were significantly lower in PAFR$^{-/-}$ mice than in wild-type mice on *day 14* after primary influenza infection and after secondary bacterial challenge; TNF-α and IL-6 levels were only trendwise lower. Because secondary pneumococcal infection resulted in a 100-fold increase in KC levels, it seems unlikely that the reduced KC levels on *day 14* after primary influenza infection contributed to the final outcome of secondary bacterial pneumonia. The reduced KC levels after secondary bacterial infection may at least in part account for the reduced neutrophil numbers in BALF, which is line with previous studies that indicate that pulmonary KC levels correlate with neutrophil influx during *S. pneumoniae* and *P. aeruginosa* infection in mice (4, 19, 27, 29). Alternatively, and not mutually exclusive, the tendency toward a reduced inflammatory response in lungs of PAFR$^{-/-}$ mice, which was also observed after primary pneumococcal pneumonia (20), could be the consequence of a lower bacterial load (providing a less potent proinflammatory stimulus) in the lungs (4).

We have previously shown that mice recovered from influenza produce high amounts of cytokines and excessive lung inflammation after induction of secondary pneumococcal pneumonia when compared with mice suffering from primary bacterial infection (30).

Because PAFR activation results in a proinflammatory stimulus, one could argue that the enhanced inflammatory reaction is partially due to PAFR expression in mice exposed to influenza. Indeed, the PAFR appears to be particularly important for the induction of pulmonary inflammation. Pretreatment with PAFR antagonists strongly diminished pulmonary vascular leakage and edema after systemic or intrapulmonary injection of lipopolysaccharide (13, 21, 23). Studies by Nagase et al. (15) revealed a critical role for the PAFR during acid aspiration in mice. Our current data argue against an important role for the PAFR in the exaggerated lung inflammation in mice with postinfluenza pneumonia, if one considers that PAFR$^{-/-}$ mice only showed a tendency toward reduced levels of proinflammatory cytokines (IL-6, TNF-α) and trendwise reduced neutrophils in their lungs. Besides, pulmonary levels of the anti-inflammatory cytokine IL-10 were modestly reduced as well. Of note, in theory, the proinflammatory properties of PAF and PAF-like lipids, such as phosphorylcholine, would make these phospholipid mediators potential protective mediators during pneumonia (2). Indeed, PAFR$^{-/-}$ mice displayed enhanced bacterial outgrowth in a mouse model for *Klebsiella pneumoniae*, a bacterium that does not express phosphorylcholine (25). This study supports the importance of phosphorylcholine binding by the PAFR during primary and secondary pneumococcal pneumonia.

S. pneumoniae is the main causative pathogen in postinfluenza pneumonia. In vitro studies have established that this bacterium can invade tissues by an interaction between phosphorylcholine present in its cell wall and the PAFR expressed by epithelial cells. We demonstrate here that the pneumococcus uses the PAFR to accomplish severe pneumonia in mice previously exposed to influenza. The fact that lethality also occurred in PAFR$^{-/-}$ mice indicates that the PAFR is not

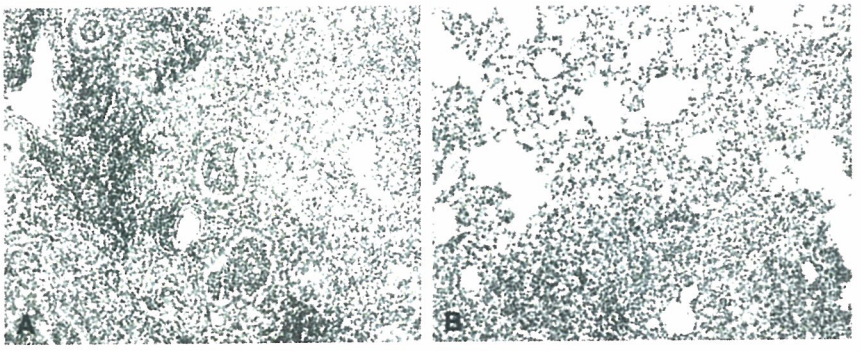

Fig. 6. Histopathological analysis. Inflammatory response upon pneumococcal infection in wild-type mice (*A*) and PAFR$^{-/-}$ mice (*B*) after recovery from influenza virus. Mice received 10^4 CFU *S. pneumoniae* on *day 14* after viral infection and were killed 48 h later. Lung slides were stained by hematoxylin and eosin (original magnification ×33). Representative slides of 6 mice per group are shown.